Biosensors and Bioelectronics ■ (■■■■) ■■■–■■■

Contents lists available at ScienceDirect

Biosensors and Bioelectronics

journal homepage: www.elsevier.com/locate/bios

Carboxyl-functionalized graphene oxide composites as SPR biosensors with enhanced sensitivity for immunoaffinity detection

Nan-Fu Chiu*, Shi-Yuan Fan, Cheng-Du Yang, Teng-Yi Huang

Laboratory of Nano-photonics and Biosensors, Institute of Electro-Optical Science and Technology, National Taiwan Normal University, No. 88, Sec. 4, Ting-Chou Road, Taipei 11677, Taiwan

ARTICLE INFO

Article history:
Received 30 November 2015
Received in revised form
20 June 2016
Accepted 22 June 2016

Keywords:
Surface plasmon resonance (SPR)
Carboxyl-functionalized graphene oxide (GO-COOH)
Immunoaffinity
Biocompatible
Biosensor

ABSTRACT

This work demonstrates the excellent potential of carboxyl-functionalized graphene oxide (GO–COOH) composites to form biocompatible surfaces on sensing films for use in surface plasmon resonance (SPR)-based immunoaffinity biosensors. Carboxyl-functionalization of graphene carbon can modulate its visible spectrum, and can therefore be used to improve and control the plasmonic coupling mechanism. The binding properties of the molecules between a sensing film and a protein were elucidated at various flow rates of those molecules. The bio-specific binding interaction among the molecules was investigated by performing an antigen and antibody affinity immunoassay. The results thus obtained revealed that the overall affinity binding value, K_A, of the Au/GO–COOH chip can be significantly enhanced by up to ~5.15 times that of the Au/GO chip. With respect to the shifts of the SPR angles of the chips, the affinity immunoassay interaction at a BSA concentration of 1 μg/ml for an Au/GO-COOH chip, an Au/GO chip and a traditional SPR chip are 35.5 m°, 9.128 m° and 8.816 m°, respectively. The enhancement of the antigen-antibody interaction of the Au/GO–COOH chip cause this chip to become four times as sensitive to the SPR angle shift and to have the lowest antibody detection limit of 0.01 pg/ml. These results indicate the potential of the chip in detecting specific proteins, and the development of real-time *in vivo* blood analysis and diagnosis based on cancer tumor markers.

1. Introduction

Graphene oxide (GO) is a new, highly malleable and highly modified carbon-based material. Its oxygen content can be reversibly reduced and increased by reduction and oxidation (Guo et al., 2009; Compton et al., 2011; Mathkar et al., 2012). The GO surface includes such oxygen-containing functional groups as epoxide groups (–O–), hydroxyl groups (–OH) and carboxylic acid groups (–COOH). Therefore, the oxygen content of GO sheets can be adjusted to provide a wide energy gap (Eda and Chhowalla, 2010; Loh et al., 2010; Johari and Shenoy, 2011; Shukla and Saxena, 2010) and non-volatile memory characteristics (Ekiz et al., 2011; Jeong et al., 2010). Research into graphene has revealed that adding compounds, such as ammonia (NH_3) (Wang et al., 2014; Li et al., 2014), boron (B) (Zhou et al., 2015; Lv et al., 2015; Dou et al., 2015), carboxylate (Sun et al., 2008; Imani et al., 2015; Liu et al., 2012; Li et al., 2013) and polymer (Chen et al., 2011; Song and Xu, 2013; Tu et al., 2014), to GO sheets readily changes their photoelectric properties, increasing their scope of application. The oxygen-containing functional groups on GO surfaces provide unique light absorption bands (Lim et al., 2012; Chang et al., 2012; Xue et al., 2014) with enhanced plasmonic coupling (Neogi et al., 2014; Niu et al., 2014) and sensitivity (Chiu and Huang, 2014; Zhao et al., 2015). These phenomena have recently been reported in relation to GO-based SPR biosensors (Chiu et al., 2014; Singh et al., 2015; Stebunov et al., 2015; Chung et al., 2015) and GO-decorated metal nanoparticle-based biosensors (Zhang et al., 2013).

In this work, GO sheets are synthesized using a modified Hummer method, yielding a carboxylate product from chloroacetic acid (Cl–CH_2–COOH) under basic conditions (Sun et al., 2008). A carboxyl-functionalized graphene oxide (GO–COOH) sheet has easily synthesized functional groups, which form unique composites. A one atom-thick planar sheet of an sp^2-bonded two-dimensional carbon material can be easily used to modulate its optical energy band gap. Covalently linked biocompatible GO–COOH composites are utilized in chemical biosensing. They can be easily modified and reused, and so are extensively used in biosensors (Song et al., 2013; Yan et al., 2015), antibacterial applications (Perreault et al., 2014), fluorescence cellular and tissue imaging (Sun et al., 2008), and anticancer drug–carrier (Imani et al., 2015) applications. The simplest means of modifying GO

* Correspondence to: Applied Science Building 3F, Institute of Electro-Optical Science and Technology, No. 88, Sec. 4, Ting-Chou Road, Wenshan Dist., Taipei 11677, Taiwan.
E-mail address: nfchiu@ntnu.edu.tw (N.-F. Chiu).

http://dx.doi.org/10.1016/j.bios.2016.06.073
0956-5663/

sheets to add carboxyl is to add carboxylate NHS ester to phosphoramidite to form a protected and activated carboxylate *in situ*. Protein amines are highly biocompatible with the biosensing film that is used in the NHS/EDC-activated carboxyl-functionalized graphene oxide reaction.

Elucidating the effect of GO–COOH-based biocompatible composites with protein on surface sensing by focal adhesion and of the use of these composites in diagnostic engineering is valuable. The optical and sensing properties of GO–COOH sheets improve the surface plasmon resonance (SPR) immunosensor sensitivity of the Au/GO–COOH chip. Carboxyl-functionalized graphene oxide composites of SPR that were developed based on an analysis of bio-interaction affinity for use as to analyze biospecific interactions. The kinetics and immunoaffinity of immobilized GO–COOH sheets can be exploited in the highly selective and specific interaction between antigen and antibody in affinity qualitative analysis.

2. Materials and methods

2.1. Preparation of immune affinity sensing films

An experiment on sensing films was performed in a series of steps. More than 80% of GO sheets that are dispersed in water comprise one atomic layer; their functional groups contain carbon (79%) and oxygen (20%). A film of modified GO sheets was synthesized as previously described (Chiu and Huang, 2014).

The GO–COOH compounds that are considered herein are organically synthesized by the interaction of graphene with chloroacetic acid under strongly basic conditions, in which the hydroxyl (–OH), epoxide (–O–), and ester groups are converted into carboxylic acid (–COOH) moieties, forming covalently linked biocompatible composites on graphene oxide surfaces (Sun et al., 2008; Štengl et al., 2014; Imani et al., 2015). The epoxide groups in the interior of the GO sheet appear to exhibit stereospecific epoxide ring-opening bonds (C–O–C). The hydroxyl groups in the interior and at the edge of the GO sheets have alkoxy bonds (C–OH), tertiary alcohol bonds (CH_3–OH), and phenolic bonds (Ar–OH). The carboxylic acid that is generated from chloroacetic acid is used to converts the epoxide groups on the basal plane of GO into hydroxyl groups, from which are formed COOH by the conjugation of acetic acid moieties, ultimately yielding GO–COOH. Following the carboxylation process, the GO is composed of both carboxyl groups at the edges and oxygenated groups in the basal planes. The GO–COOH sheets were dispersed in aqueous solution (0.275 g/l, 10 ml) with shattering by ultra-sonication for 2 h. Therefore, the hydrophilic functional groups, including –COOH and –OH, were exposed on the GO basal planes in a process that is similar to the organic matrix-mediated biomineralization of mollusk shells (Okhrimenko et al., 2013; Li et al., 2015). Fig. 1(a) presents the chemical structures of the surfaces of the GO-COOH sheets.

A sensing chip was prepared from a 47 nm-thick film of gold (Au) and a 2 nm-thick chromium (Cr) adhesion layer, which was deposited by an electron beam evaporator on a high-performance BK7 substrate (Chiu and Huang, 2014; Chang et al., 2010). An Au film that was chemically modified using a derivatized thiol self-assembled monolayer (SAM) of cystamine (Cys, cystamine dihydrochloride 96%) was prepared by immersing an Au film in an ethanol solution of Cys (5 mM) for 24 h at room temperature. An *in situ* method for preparing GO-COOH sheets involved immobilization onto Au film. The Au film was prepared by immersing in aqueous GO–COOH (0.275 g/l) for 5 h. Deionized water was used to rinse the Au film to remove any non-immobilized GO-COOH sheets. The remaining GO-COOH sheets were adsorbed onto the Au-linker surfaces. Fig. 1(b) schematically depicts the fabrication of GO–COOH sheets in an Au film. The GO–COOH sheets thus becomes part of an Au/Cys(5 mM)/GO–COOH(0.275 g/l) chip structure. A GO sheet is fabricated for using in another sensing chip for use in a comparative experiment. The Au film was prepared by immersing in aqueous GO (2 g/l) for 5 h. Deionized water was used to rinse the Au film to remove any non-immobilized GO sheets.

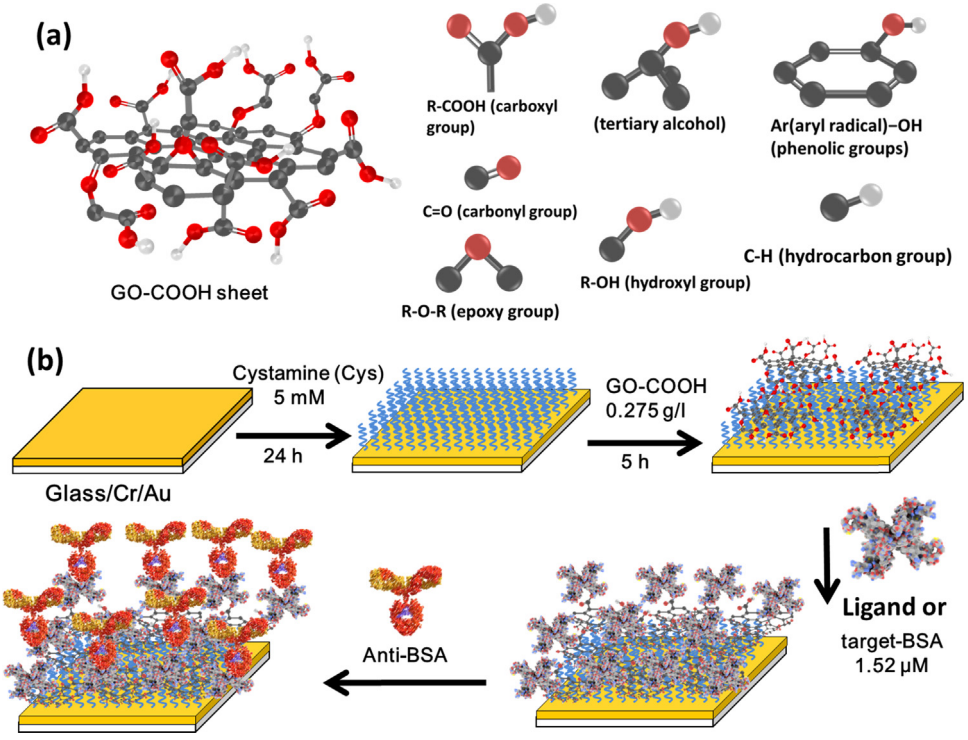

Fig. 1. (a) Molecular structure of carboxyl-functionalized GO sheet and its oxygen-containing functional groups. (b) Fabrication of SPR chip with bio-molecular immobilization on modified surface of carboxyl-functionalized GO film.

Please cite this article as: Chiu, N.-F., et al., Biosensors and Bioelectronics (2016), http://dx.doi.org/10.1016/j.bios.2016.06.073

The GO sheet thus formed was used in a sensing chip with an Au/Cys(5 mM)/GO(2 g/l) structure (Chiu et al., 2014).

2.2. Models of immunoaffinity biosensors and execution of detection program

The carboxyl end groups on the surfaces of the formed GO–COOH sheets were activated by injecting a mixture of 0.1 mM N-hydroxysuccinimide (NHS) and 0.4 mM N-ethyl-3-(3-dimethylaminopropyl) carbodiimide (EDC) in a 1:1 ratio into phosphate-buffered saline (PBS) at pH 7.2–7.5 for 10 min, after injecting 200 µl of the mixture into a dual-channel microfluidics SPR BI-3000 system. GO–COOH sheets that are immobilized on EDC/NHS-crosslinks can be used to prepare chemically modified terminal groups (–COOH) by surface-confined ester reactions. The activated GO–COOH surface undergoes strongly covalent immobilization by an amine (NH_2)-coupling reaction in a protein ligand or bovine serum albumin (BSA) protein. Then, phosphate-buffered saline (PBS) solution acted as a running buffer and was utilized to wash these non-binding protein molecules from the sensor film to establish the immobilized capturing protein molecule and the baseline levels of the detection target protein BSA. To block the potential sites of the interaction, 1 M ethanolamine (EA) solution is injected into the microfluidics system. Assays for detecting protein in a dual-microfluidic channel involve SPR angular modulation. All experiments herein were conducted at room temperature, using a sample injection volume of 200 µl and a flow rate of 60 µl/min. Results were repeatedly obtained by the same chip detection method using various sensing channel paths.

3. Results and discussion

3.1. Surface analysis and properties of sensing films

Large-area carboxyl-functionalized GO films with uniform thickness were modified. Fig. 2 presents SEM images of the GO–COOH films that were formed when 0.275 g/l carboxyl-functionalized GO solution was immobilized on the surface of an Au electrode by covalent bonds. Then, the GO–COOH sheets were broken up into strips of size 0.1–1 µm. In the carboxyl-functionalization process, carboxylic acids turned the GO surface into an organic matrix with hydrophilic functional groups (Li et al., 2015). This process is a critical in the replacement of traditional SPR chips with highly sensitive biosensors with a high affinity for biomolecules.

3.2. Optical properties of carboxyl-functionalized graphene oxide

Fig. 3(a) presents the Fourier transform infrared (FTIR) spectra of Au/GO chip and Au/GO–COOH chip in attenuated total reflection (ATR) mode, which were analyzed to prove GO–COOH bonds on the surface of the Au film and to elucidate the properties of various oxygenated species. The successful carboxyl-functionalization of GO sheets were synthesized and the ionizable –COOH continuously and densely covers the surface of a sensing film. All absorption bands can be observed in the FTIR spectra. Fig. 3 (a) indicates that GO–COOH has a clear band around 1660 cm^{-1} that corresponds to the vibration of (–COOH) carbonyl (Acik et al., 2010), a band around 1735 cm^{-1} that corresponds to the vibration of C=O (Toh et al., 2014), a band around 1535 cm^{-1} that corresponds to the vibration of C=C (Acik et al., 2010), a band around 1375 cm^{-1} that corresponds to the vibration of tertiary alcohol (Loh et al., 2010), a band around 1265 cm^{-1} that corresponds to the asymmetric vibration of (C–O–C) epoxide (Acik et al., 2010), a band around 1080 cm^{-1} that corresponds to the vibration of (C–O) alkoxy, and a band around 850 cm^{-1} that corresponds to the vibration of (C–O–C) epoxide (Acik et al., 2010). A comparison between GO and GO–COOH sheets clearly reveals that the latter yields must larger carbonyl peaks (1660 cm^{-1}). Furthermore, a broad band peak that corresponds to the vibration of –OH (3200–3640 cm^{-1}) (Toh et al., 2014) is observed at large wave-numbers, along with a CH_2 peak at 2851 cm^{-1} and a CH_2 peak at 2920 cm^{-1} (Lai et al., 2011; John et al., 2000; Berg and Klenerman, 2003). Therefore, Fig. 3(a) reveals significant reductions in the hydroxyl (–OH), epoxide (–O–) groups contents, confirming the carboxyl-functionalization of GO sheets is successful. Figs. S1 and S2 (supplementary) present X-Ray photoelectron spectroscopy (XPS) analyses of Au/GO and Au/CO-COOH chips. The successful carboxyl-functionalization of GO sheets is observed and GO-COOH bonds to the surface of the Au film.

Fig. 3(b) presents the ultraviolet–visible (UV–vis) absorption spectra of aqueous GO sheets at concentrations of 0.1 g/l and 0.275 g/l and aqueous GO–COOH sheets at a concentration of 0.275 g/l. The absorption spectra of the GO sheets were higher than those of the GO–COOH sheets. GO yielded two absorption peaks: the maximum at 235 nm corresponds to the π-π^* transitions of aromatic C–C bonds in variously sized aromatic sp2 clusters, and the shoulder at 295 nm is attributable to n-π^* transitions that are caused by the presence of epoxide and carbonyl (C=O) bonds (Li et al., 2012; Yang et al., 2012). GO at a high concentration of 0.275 g/l yielded a strong Soret peak at 415 nm (Tu et al., 2010; Guo et al., 2011) with a range of absorption of 350–530 nm. The Soret band arises from the through-space exciton coupling

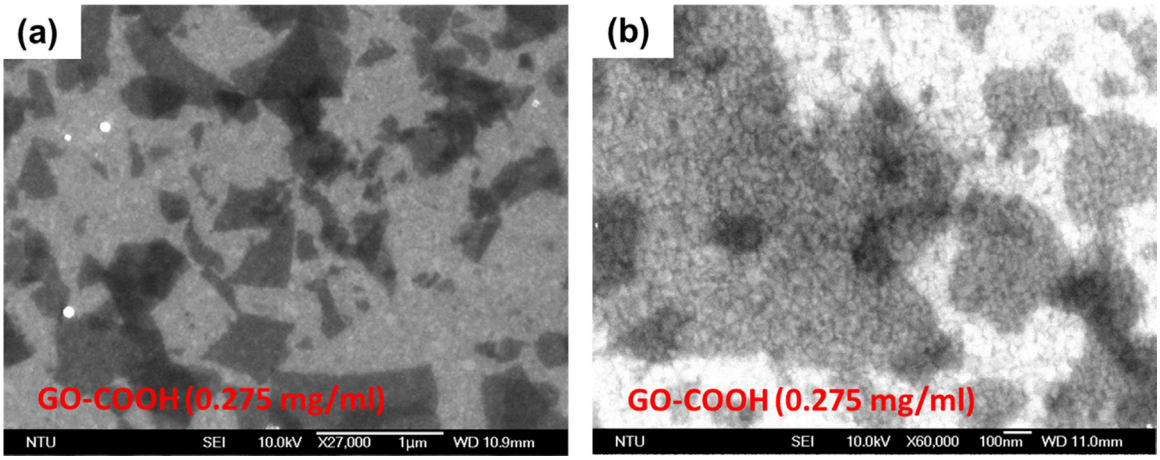

Fig. 2. SEM images of as-prepared carboxyl-functionalized graphene oxide sheet at various magnifications.

Please cite this article as: Chiu, N.-F., et al., Biosensors and Bioelectronics (2016), http://dx.doi.org/10.1016/j.bios.2016.06.073

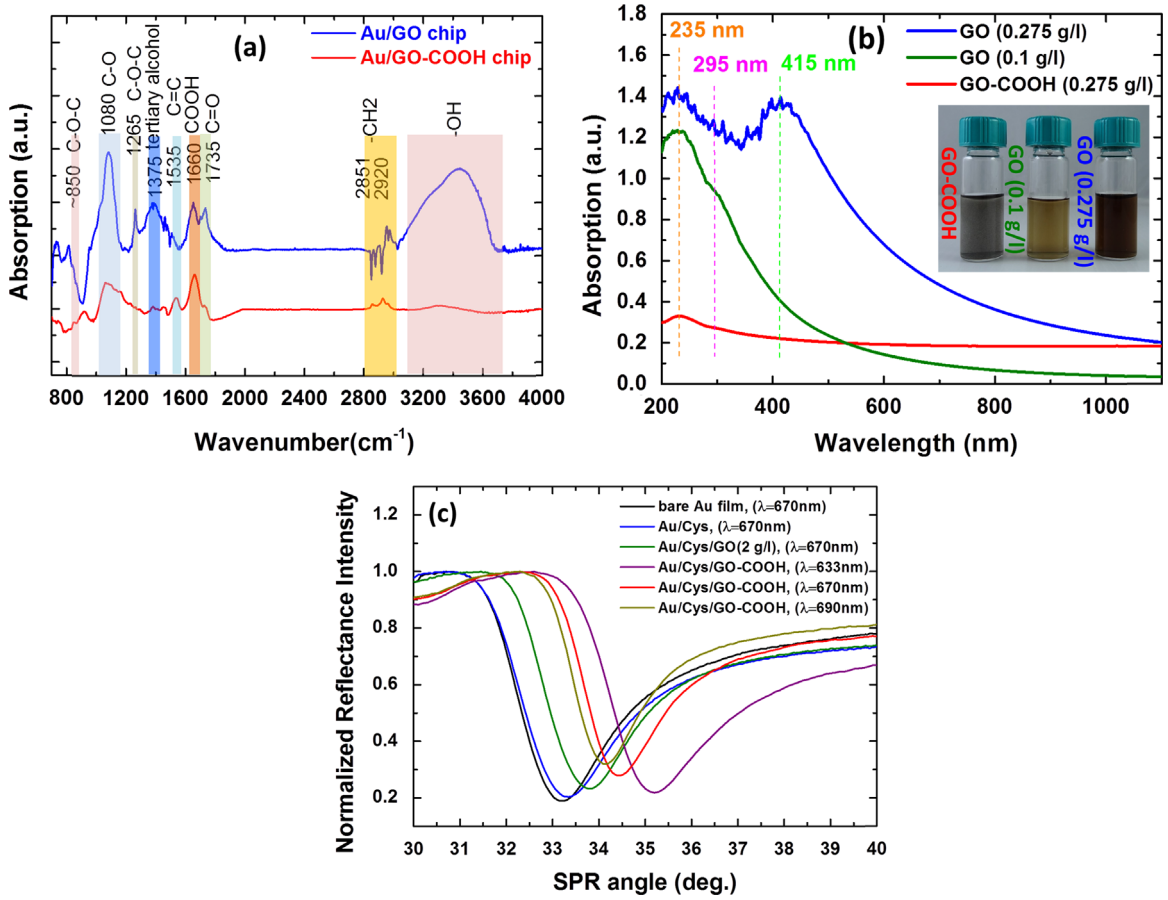

Fig. 3. (a) FTIR spectra of GO and GO–COOH films; (b) UV–vis absorption spectra of GO (0.275 g/l) and GO–COOH (0.275 g/l) for incident wavelengths from 190 nm to 1100 nm (Inset: photographic images of GO and GO–COOH solutions); (c) SPR reflection absorption spectra of sensing chips.

interaction between the oxygen π-band and the carbon π-bands movement of dipoles that allow π-π* transitions.

Fig. 3(c) presents the SPR angle spectra for a Kretschmann configuration on various sensing chips, including bare Au, Au/Cys, Au/Cys/GO and Au/Cys/GO–COOH, under incident light at wavelengths of 633, 670 and 690 nm in air as the surrounding medium. The figure reveals that the refractive index varies with the thickness of the film, and the SPR angle shifts are 33.2° for a bare Au chip, 33.35° for an Au/Cys chip, 33.8° for an Au/Cys/GO chip and 34.1°, 34.4° and 35.2° for an Au/GO–COOH chip with incident wavelengths of 633 nm, 670 nm and 690 nm, respectively. Accordingly, GO and GO–COOH sheets were successfully adsorbed on the surfaces of the Au/Cys films. Since the carboxyl-functionalized GO films were immobilized at the Au surface, a Au/GO-COOH chip has a large surface area for the efficient covalent immobilization of biomolecules. The films have a thickness of the same order of magnitude as the penetration depth of the evanescent wave.

3.3. Bonding and molecular dynamics in biological interactions

Fig. 4(a-c) presents the bonding force between the sensing film and BSA protein. Two chips, the Au/GO–COOH chip and the Au/GO chip, are compared. In the test, the target protein, at a concentration of 100 μg/ml and a volume of 200 μl, was injected into microfluidics. The SPR curve plots the relationship between the sensing film and the detection target protein of the interactions with the sensing film at various injected flow rates, elucidating the binding kinetics of BSA protein. The negatively charged carboxyl groups in the Au/GO–COOH chip are usually required to interact electrostatically with positively charged analytes in solution as well the protein during the immobilization process. The covalent attachment of GO–COOH sheets and BSA molecules provides a hydrophilic environment that is favorable to most solution-based biomolecular interactions. Based on the SPR sensorgram that was obtained for kinetic analysis, the affinity binding constants (K_A) that characterize the interactions of BSA molecules are calculated from the association rate constant and the dissociation rate constant using the relation $K_A = k_a/k_d$ (Chiu et al., 2014). The shifts in SPR angle for the Au/GO chip and the Au/GO–COOH chip at equilibrium were 118.05 and 119.35 m° (m°=milli degree), respectively, at a flow rate of 30 μl/min; 115.09 and 143.62 m° at a flow rate of 60 μl/min, and 83.15 and 90.43 m° at flow rate of 90 μl/min. Fig. 4(a) and (c) present the molecule bonding force and kinetic coefficient of the BSA protein, revealing a non-optimal response of the SPR angle shift to the Au/GO chip or the Au/GO–COOH chip at flow rates of 30 and 90 μl/min. Table 1 presents the calculated kinetic coefficients for the molecular bonding reaction.

Fig. 4(a) and (b) reveal that jitter in the temporal response of the SPR sensorgram during dissociation of the target protein BSA from the carboxyl-functionalized chip was a non-specific binding phenomenon (supplementary content), which was caused by the fact that high (saturation) concentrations of carboxyl functional groups were present on GO surfaces.

Fig. 4(b) presents the Au/GO–COOH chip. Kinetic analyses yielded an affinity binding constant, K_A, of $413.93 \times 10^6\ M^{-1}$ and a dissociation constant, K_D, of 2.42×10^{-9} M. At a flow rate of 60 μl/min, the Au/GO–COOH chip exhibited high affinity for the sensing film in the bonding reaction of the target BSA protein molecules. The ratio of the affinity binding constants, K_A, of Au/GO chip to that of the Au/GO–COOH chip was 1:5.15. The corresponding ratio

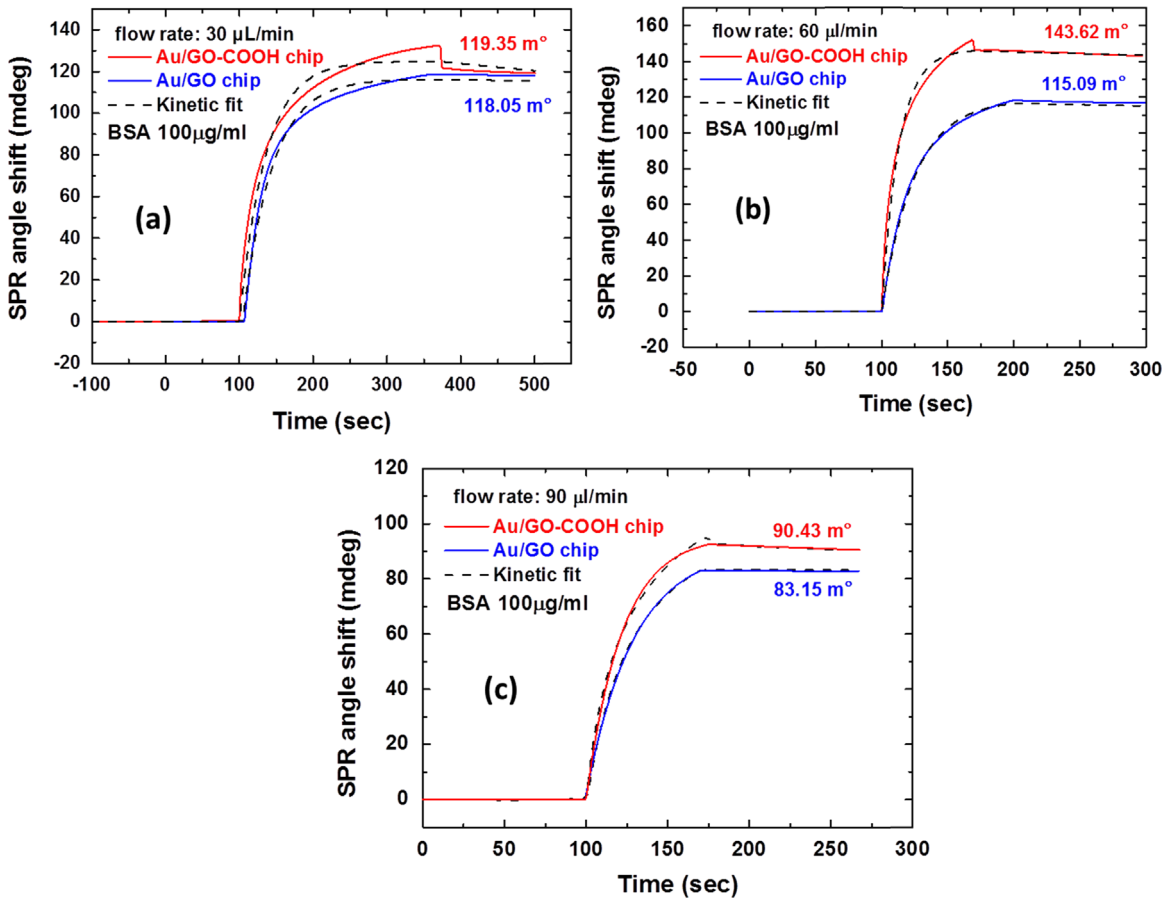

Fig. 4. SPR sensorgrams obtained during bonding reaction between biological molecules and sensing interface, showing kinetic coefficients at flow rates of (a) 30 μl/min (b) 60 μl/min and (b) 90 μl/min.

Table 1
Affinity and rate constants for kinetic binding/unbinding of sensing film and protein.

Type of chip (flow rate)	SPR angle (m°)	k_a (10^4 M^{-1} S^{-1})	k_d (10^{-4} S^{-1})	K_A (10^6 M^{-1})	K_D (10^{-9} M)
Au/GO (30 μl/min)	118.05	1.53	3.48	44.02	22.72
Au/GO–COOH (30 μl/min)	117.18	1.86	2.85	65.26	15.32
Au/GO (60 μl/min)	115.09	2.66	3.31	80.36	12.44
Au/GO–COOH (60 μl/min)	143.62	5.05	1.22	413.93	2.42
Au/GO (90 μl/min)	83.15	2.07	3.16	65.44	15.28
Au/GO–COOH (90 μl/min)	94.09	3.02	2.36	127.96	7.8

k_a is the association rate constant, k_d is the dissociation rate constant.
K_A is the binding constant, K_D is the dissociation constant.

of the resonance angle shifts was 1:1.25. The experimental results indicate that the sensing of GO–COOH chip is superior to that by other sensing chips, and that the former exhibits a very high sensitivity. The target protein BSA was demonstrated to interact strongly with the GO–COOH film.

3.4. Affinity antibody-antigen recognition with biomolecular interaction analysis

Fig. 5(a) the real-time SPR sensorgram, which reflects the various concentrations of accumulated antigen-antibody interactions in the Au/GO–COOH and Au/GO chip surfaces. The antibody-BSA exhibits specific adsorption from low to high concentrations, almost reaching saturation in the affinity interaction.

The ratios of the shifts in the resonance angle of the Au/GO–COOH chip to that of the Au/GO chip in anti-BSA at concentrations of 100 μg/ml, 50 μg/ml, 25 μg/ml, 10 μg/ml, 5 μg/ml and 1 μg/ml were 2.76, 2.97, 3.37, 3.03, 4.06, and 3.89, respectively. These results corresponded to shifts in the SPR angle at equilibrium of 470.33 m°, 428.23 m°, 364.89 m°, 184.8 m°, 123.88 m° and 35.5 m°, respectively.

The results clearly indicating that the Au/GO–COOH chip exhibits excellent detection sensitivity. The exponential regression of the calibration curve yielded $y=463.87–450.67e^{-0.05x}$ and $R^2=0.997$ for the Au/GO–COOH chip, $y=171.18–168.81e^{-0.04x}$ and $R^2=0.995$ for the Au/GO chip, and $y=83.59–76.42e^{-0.05x}$ and $R^2=0.993$ for the traditional SPR chip, where x denotes the refractive concentration and y is the SPR angle, as presented in Fig. 5 (b). The experimental data in the Au/GO–COOH chip were highly consistent with the calibration curve.

Fig. 5(c) compares the sensitivities of three sensing chips to antibody-BSA at a concentration of 1 μg/ml and a flow rate of 60 μl/min in terms of the SPR angle shift.

The results obtained in an anti-BSA concentration of 1 μg/ml

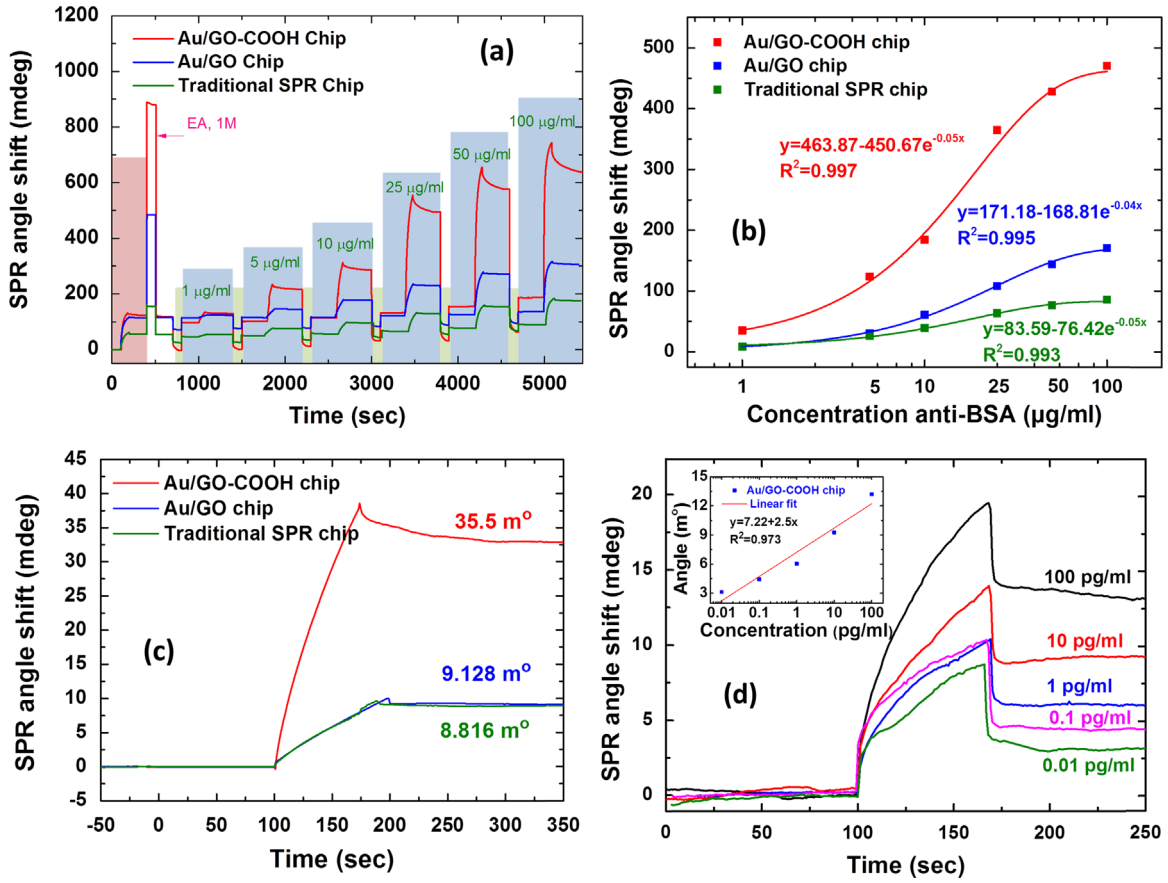

Fig. 5. SPR analysis of interaction of antibody-BSA with immobilized antigen (BSA) on sensing chip. Shifts of SPR angle due to antigen-antibody immunoreaction were measured in real-time. (a) Obtained from six cycles of analysis of antigen-antibody interaction on various sensing chips with various analyte concentrations. Red, blue and green lines represent SPR sensorgrams of Au/GO-COOH chip, Au/GO chip and traditional chip, respectively. (b) The calibration curve is obtained by plotting the SPR angle shift as a function of concentration of anti-BSA; it is used in the equilibrium analysis of the binding of anti-BSA protein to a high-affinity BSA protein. (c) The sensorgram was obtained in the SPR angle shift, at the anti-BSA concentration of 1 μg/ml. (d) The Au/GO-COOH chip herein had an anti-BSA concentration ultra-low detection limit of as low as 0.01 pg/ml. The inset shows a calibration curve that reveals high sensitivity and a large range of linearity. (For interpretation of the references to color in this figure legend, the reader is referred to the web version of this article.)

indicated shifts in the SPR angle for the traditional SPR chip, the Au/GO chip and the Au/GO–COOH chip at equilibrium of 8.816 m°, 9.128 m° and 35.5 m°, respectively. The Au/GO–COOH chip exhibited high an affinity for 1 μg/ml anti-BSA, with four times the shift in the SPR angle of the other chip. The obtained results reveal that the Au/GO–COOH chip was highly sensitive to low concentrations of anti-BSA.

Fig. 5(d) presents the lower limit on quantitation, which is equivalent to sensitivity, as well as the limit of detection (LOD), of the Au/GO–COOH chip. The LOD is 0.01 pg/ml for the anti-BSA sample, as presented in Fig. 5(d). The inset shows the calibration plot for the Au/GO–COOH chip, which reveals that the range of linearity is 0.01–100 pg/ml. The linear regression of the calibration curve for the Au/GO–COOH chip yields $y=7.22+2.5x$ and $R^2=0.973$. The responsivities of the SPR angle curve in the range of linearity and the calibration curves clearly reveal that the Au/GO–COOH chip was more sensitive than the other sensing chips. The experimental results demonstrate that the carboxyl-functionalized graphene oxide sensing chip exceeded the traditional chip detection limit.

4. Conclusions

An SPR-based biosensor that was based on carboxyl-functionalized graphene oxide composites was developed; it had a large area, a strong binding reaction with biomolecules and a high affinity for specificity assessment in immunoassay because carboxyl-modified graphene oxide has a high specific surface area, and therefore very high biocompatibility. Linear regression analysis reveals high reproducibility and a strongly linear relationship with a correlation coefficient of 0.973 at concentrations of 0.01–100 pg/ml for the calibration curve due to the Au/GO–COOH chip exhibits excellent detection sensitivity. Experimental results revealed that the Au/GO–COOH chip had by far the lowest detection limit, compared to Au/GO and traditional SPR chip of 0.01 pg/ml. We believe that this work will support the development of excellent biosensors and elucidates an exciting approach to using carboxyl-modified graphene oxide in highly sensitive and selective biosensors as alternatives to traditional sensing films. The results in this study will contribute to the future detection of specific proteins; they are of particular value in early detection and diagnosis in the field of medicine, as well as the development of immunosensors for specific affinity antibody-antigen recognition analysis.

Acknowledgements

The authors would like to thank the Ministry of Science and Technology of the Republic of China, Taiwan, for financially supporting this research under Contract No. MOST 103-2221-E-003 -008, NSC 102-2221-E-003-021, and NSC 99-2218-E-003-002-

MY3. We thank Dr. Yao-Jane Hsu, Dr. Ming-Wei Lin and Yu-Ling Lai for they help in analyzing XPS spectra (National Synchrotron Radiation Research Center, Beamline 09A2) and Instrumentation Center at National Tsing Hua University (FTIR) provided support for this work.

Appendix A. Supplementary material

Supplementary data associated with this article can be found in the online version at http://dx.doi.org/10.1016/j.bios.2016.06.073.

References

Acik, M., Lee, G., Mattev, C., Chhowalla, M., Cho, K., Chabal, Y.J., 2010. Unusual infrared-absorption mechanism in thermally reduced graphene oxide. Nat. Mater. 9, 840–845.
Berg, O., Klenerman, D., 2003. Vibrational spectroscopy of mechanically compressed monolayers. J. Am. Chem. Soc. 125, 5493–5500.
Chang, C.-C., Chiu, N.-F., Lin, D.S., Chu, S.-Y., Lin, C.-W., 2010. High-sensitivity detection of carbohydrate antigen 15-3 using a gold/zinc oxide thin films surface plasmon resonance–based biosensor. Anal. Chem. 82, 1207–1212.
Chang, L., Chen, S., Jin, P., Li, X., 2012. Synthesis of multifunctional fluorescent magnetic graphene oxide hybrid materials. J. Colloid Interface Sci. 388, 09–14.
Chen, B., Liu, M., Zhang, L., Huang, J., Yao, J., Zhang, Z., 2011. Polyethylenimine-functionalized graphene oxide as an efficient gene delivery vector. J. Mater. Chem. 21, 7736–7741.
Chiu, N.-F., Huang, T.-Y., 2014. Sensitivity and kinetic analysis of graphene oxide-based surface plasmon resonance biosensors. Sens. Actuators B 197, 35–42.
Chiu, N.-F., Huang, T.-Y., Lai, H.-C., Liu, K.-C., 2014. Graphene oxide-based SPR biosensor chip for immunoassay applications. Nanoscale Res. Lett. 9, 445–451.
Chung, K., Rani, A., Lee, J.E., Kim, J.E., Kim, Y., Yang, H., Kim, S.O., Kim, D., Kim, D.H., 2015. Systematic study on the sensitivity enhancement in graphene plasmonic sensors based on layer-by-layer self-assembled graphene oxide multilayers and their reduced analogues. ACS Appl. Mater. Interfaces 7, 144–151.
Compton, O.C., Jain, B., Dikin, D.A., Abouimrane, A., Amine, K., Nguyen, S.T., 2011. Chemically active reduced graphene oxide with tunable C/O ratios. ACS Nano 5 (6), 4380–4391.
Dou, S., Huang, X., Ma, Z., Wu, J., Wang, S., 2015. A simple approach to the synthesis of BCN graphene with high capacitance. Nanotechnology 26, 045402–045409.
Eda, G., Chhowalla, M., 2010. Chemically derived graphene oxide: towards large-area thin-film electronics and optoelectronics. Adv. Mater. 22, 2392–2415.
Ekiz, O.O., Urel, M., Guner, H., Mizrak, A.K., Dana, A., 2011. Reversible electrical reduction and oxidation of graphene oxide. ACS Nano 5 (4), 2475–2482.
Guo, C.X., Lei, Y., Li, C.M., 2011. Porphyrin functionalized graphene for sensitive electrochemical detection of ultratrace explosives. Electroanalysis 23 (4), 885–893.
Guo, H.-L., Wang, X.-F., Qian, Q.-Y., Wang, F.-B., Xia, X.-H., 2009. A green approach to the synthesis of graphene nanosheets. ACS Nano 3 (9), 2653–2659.
Imani, R., Emami, S.H., Faghihi, S., 2015. Synthesis and characterization of an octaarginine functionalized graphene oxide nano-carrier for gene delivery applications. Phys. Chem. Chem. Phys. 17, 6328–6339.
Jeong, H.Y., Kim, J.Y., Kim, J.W., Hwang, J.O., Kim, J.-E., Lee, J.Y., Yoon, T.H., Cho, B.J., Kim, S.O., Ruoff, R.S., Choi, S.-Y., 2010. Graphene oxide thin films for flexible nonvolatile memory applications. Nano Lett. 10, 4381–4386.
Johari, P., Shenoy, V.B., 2011. Modulating optical properties of graphene oxide: role of prominent functional groups. ACS Nano 5 (9), 7640–7647.
John, S.A., Kitamura, F., Tokuda, K., Ohsaka, T., 2000. Can N-ethyl-N%-octadecyl viologen dimerize on octadecanethiol-coated gold electrode? Electrochim. Acta 45, 4041–4048.
Lai, F., Pini, E., Angioni, G., Manca, M.L., Perricci, J., Sinico, C., Fadda, A.M., 2011. Nanocrystals as tool to improve piroxicam dissolution rate in novel orally disintegrating tablets. Eur. J. Pharm. Biopharm. 79 (3), 552–558.
Li, Q., Fan, F., Wang, Y., Feng, W., Ji, P., 2013. Enzyme immobilization on carboxyl-functionalized graphene oxide for catalysis in organic solvent. Ind. Eng. Chem. Res. 52, 6343–6348.
Li, D., Yu, D., Wang, M., Zhang, Y., Pan, C., 2014. Synthesis of nitrogen doped graphene from graphene oxide within an ammonia flame for high performance supercapacitors. RSC Adv. 4, 55394–55399.
Li, J., Liu, C.-y, Liu, Y., 2012. Au/graphene hydrogel: synthesis, characterization and its use for catalytic reduction of 4-nitrophenol. J. Mater. Chem. 22, 8426–8430.
Li, J., Liu, D., Li, B., Wang, J., Han, S., Liu, L., Wei, H., 2015. A bio-inspired nacre-like layered hybrid structure of calcium carbonate under the control of carboxyl graphene. CrystEngComm 17, 520–525.
Lim, S.Y., Ahn, J., Lee, J.S., Kim, M.-G., Park, C.B., 2012. Graphene-oxide-based immunosensing through fluorescence quenching by peroxidase-catalyzed polymerization. Small 8 (13), 1994–1999.
Liu, Y., Deng, R., Wang, Z., Liu, H., 2012. Carboxyl-functionalized graphene oxide-polyaniline composite as a promising supercapacitor material. J. Mater. Chem. 22, 13619–13624.
Loh, K.P., Bao, Q., Eda, G., Affiliations, M.C., 2010. Graphene oxide as a chemically tunable platform for optical applications. Nat. Chem. 2, 1015–1024.
Lv, R., Chen, G., Li, Q., McCreary, A., Botello-Méndez, A., Morozov, S.V., Liang, L., Declerck, X., Perea-López, N., Cullen, D.A., Feng, S., Elías, A.L., Cruz-Silva, R., Fujisawa, K., Endo, M., Kang, F., Charlier, J.-C., Meunier, V., Pan, M., Harutyunyan, A.R., Novoselov, K.S., Terrones, M., 2015. Ultrasensitive gas detection of large-area boron-doped graphene. PNAS 112 (47), 14527–14532.
Mathkar, A., Tozier, D., Cox, P., Ong, P., Galande, C., Balakrishnan, K., Reddy, A.L.M., Ajayan, P.M., 2012. Controlled, stepwise reduction and band gap manipulation of graphene oxide. J. Phys. Chem. Lett. 3, 986–991.
Neogi, A., Karna, S., Shah, R., Phillipose, U., Perez, J., Shimada, R., Wang, Z.M., 2014. Surface plasmon enhancement of broadband photoluminescence emission from graphene oxide. Nanoscale 6, 11310–11315.
Niu, W., Chen, H., Chen, R., Huang, J., Palaniappan, A., Sun, H., Liedberg, B.G., Tok, A.I. Y., 2014. Synergistically enhanced near-infrared photoresponse of reduced graphene oxide by upconversion and gold plasmon. Small 10 (18), 3637–3643.
Okhrimenko, D.V., Nissenbaum, J., Andersson, M.P., Olsson, M.H.M., Stipp, S.L.S., 2013. Energies of the adsorption of functional groups to calcium carbonate polymorphs: the importance of –OH and –COOH groups. Langmuir 29 (35), 11062–11073.
Perreault, F., Tousley, M.E., Elimelech, M., 2014. Thin-film composite polyamide membranes functionalized with biocidal graphene oxide nanosheets. Environ. Sci. Technol. Lett. 1 (1), 71–76.
Shukla, S., Saxena, S., 2010. Spectroscopic investigation of confinement effects on optical properties of graphene oxide. Appl. Phys. Lett. 98, 073104.
Singh, M., Holzinger, M., Tabrizian, M., Winters, S., Berner, N.C., Cosnier, S., Duesberg, G.S., 2015. Noncovalently functionalized monolayer graphene for sensitivity enhancement of surface plasmon resonance immunosensors. J. Am. Chem. Soc. 137, 2800–2803.
Song, M., Xu, J., 2013. Preparation of polyethylenimine-functionalized graphene oxide composite and Its application in electrochemical ammonia sensors. Electroanalysis 25 (2), 523–530.
Song, E., Cheng, D., Song, Y., Jiang, M., Yu, J., Wang, Y., 2013. A graphene oxide-based FRET sensor for rapid and sensitive detection of matrix metalloproteinase 2 in human serum sample. Biosens. Bioelectron. 47, 445–450.
Stebunov, Y.V., Aftenieva, O.A., Arsenin, A.V., Volkov, V.S., 2015. Highly sensitive and selective sensor chips with graphene-oxide linking layer. ACS Appl. Mater. Interfaces 7, 21727–21734.
Štengl, V., Bakardjieva, S., Bakardjiev, M., Štíbr, B., Kormunda, M., 2014. Carborane functionalized graphene oxide, a precursor for conductive self-assembled monolayers. Carbon 67, 336–343.
Sun, X., Liu, Z., Welsher, K., Robinson, J.T., Goodwin, A., Zaric, S., Dai, H., 2008. Nano-graphene oxide for cellular imaging and drug delivery. Nano Res. 1 (3), 203–212.
Tu, Q., Pang, L., Chen, Y., Zhang, Y., Zhang, R., Lu, B., Wang, J., 2014. Effects of surface charges of graphene oxide on neuronal outgrowth and branching. Analyst 139, 105–115.
Toh, S.Y., Loh, K.S., Kamarudin, S.K., Daud, W.R.W., 2014. Graphene production via electrochemical reduction of graphene oxide: Synthesis and characterization. Chem. Eng. J. 251, 422–434.
Tu, W., Lei, J., Zhang, S., Ju, H., 2010. Characterization, direct electrochemistry, and amperometric biosensing of graphene by noncovalent functionalization with picket-fence porphyrin. Chem. Eur. J. 16, 10771–10777.
Wang, Y., Zhang, L., Hu, N., Wang, Y., Zhang, Y., Zhou, Z., Liu, Y., Shen, S., Peng, C., 2014. Ammonia gas sensors based on chemically reduced graphene oxide sheets self-assembled on Au electrodes. Nanoscale Res. Lett. 9, 251–263.
Xue, T., Cui, X., Guan, W., Wang, Q., Liu, C., Wang, H., Qi, K., Singh, D.J., Zheng, W., 2014. Surface plasmon resonance technique for directly probing the interaction of DNA and graphene oxide and ultra-sensitive biosensing. Biosens. Bioelectron. 58, 374–379.
Yan, F., Zhang, Y., Zhang, S., Zhao, J., Liu, S., He, L., Feng, X., Zhang, H., Zhang, Z., 2015. Carboxyl-modified graphene for use in an immunoassay for the illegal feed additive clenbuterol using surface plasmon resonance and electrochemical impedance spectroscopy. Microchim. Acta 182, 855–862.
Yang, S., Yue, W., Huang, D., Chen, C., Lin, H., Yang, X., 2012. A facile green strategy for rapid reduction of graphene oxide by metallic zinc. RSC Adv. 2, 8827–8832.
Zhang, J., Sun, Y., Xu, B., Zhang, H., Gao, Y., Zhang, H., Song, D., 2013. A novel surface plasmon resonance biosensor based on graphene oxide decorated with gold nanorod–antibody conjugates for determination of transferrin. Biosens. Bioelectron. 45, 230–236.
Zhou, Y., Yen, C.H., Fu, S., Yang, G., Zhu, C., Du, D., Wo, P.C., Cheng, X., Yang, J., Wai, C. M., Lin, Y., 2015. One-pot synthesis of B-doped three-dimensional reduced graphene oxide via supercritical fluid for oxygen reduction reaction. Green Chem. 17, 3552–3560.
Zhao, Y., Zeng, W., Tao, Z., Xiong, P., Qucd, Y., Zhu, Y., 2015. Highly sensitive surface-enhanced Raman scattering based on multi-dimensional plasmonic coupling in Au–graphene–Ag hybrids. Chem. Commun. 51, 866–869.